Penerbit Akademia Baru

Journal of Advanced Research in Fluid Mechanics and Thermal Sciences

Journal homepage: www.akademiabaru.com/arfmts.html
ISSN: 2289-7879

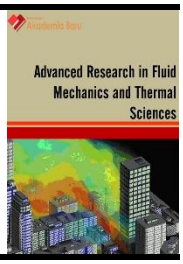

Nanobubbles Interaction on Flat Plates Affecting Volumetric Gas Flux and Local Void Ratio

Open Access

Yanuar[1,*], Gunawan[1], A. S. A. Utomo[1]

[1] Department of Mechanical Engineering, Faculty of Engineering, Universitas Indonesia, Depok 16424, Indonesia

ARTICLE INFO

Article history:
Received 17 December 2019
Received in revised form 14 January 2020
Accepted 14 January 2020
Available online 9 April 2020

Keywords:
Nanobubble; boundary layer; multiplier constants; volumetric flux; plate spacing

ABSTRACT

A pipe has a great significance to deposit fluid from one place to another. Distributing solution to the engine, cooling system, and ballast system are crucial for a ship to operate correctly. Drag is one of the obstructions in the internal flow of the pipeline, restricting the fluid to stream smoothly. Majority studies use numerous methods to reduce the effect, such as using microbubble, minimizing the length of pipe installation, and injection of nanobubble. Bubble drag reduction is one of the most modern methods; the previous study showed that 2mm bubble size has a lot less beneficial for decreasing drag than a 40 µm bubble at the same fluid velocity. Based on previous research, this study will show the impact of nanobubble in reducing drag produced by a carbon-ceramic nozzle. This research studies the nanobubble influence explicitly by using diverge types of conditions such as various injection distance, several areas of the plates, and analyze the utilization of nanobubble and microbubble within the boundary layer. The boundary layer investigated by circumscribing volumetric gas flux and gas flux injection and then scrutinize the findings providing a local void ratio. Research towards the boundary layer used a shred of photographic evidence, examine by using Jimage processing to view the distance between the exterior of the plates and the current generated by nanobubble injection. Flux ratio created from the resulting multiplier constant, which is the ß factor that expresses the effectiveness of the nanobubble drag reduction technique. Finally, the result obtained that nanobubble is 0.82912 times more efficient than using microbubble with an injection range of 80mm and a local void ratio of 2.1.

Copyright © 2020 PENERBIT AKADEMIA BARU - All rights reserved

1. Introduction

According to H. Sayyaadi *et al.,* [1], there are two groups of drag, i.e., viscous and pressure drag. Viscous drag is a force that emerges within the crossing of two objects. In contrast, pressure drag is a result of both exteriors when a particular pair of objects met. Diminishing drag associated with various techniques introduced by numerous experiments conducted by Madavan *et al.,* [2] and

* *Corresponding author.*
E-mail address: yanuar@eng.ui.ac.id (Yanuar)

https://doi.org/10.37934/arfmts.69.1.137147

Kodama *et al.,* [3], it confers immense commercial impact, such as delivering higher performance ships with lubrication methods. However, the use of micro-sized bubbles has several limitations, such as the features of microbubbles that can encounter slippage because it can not exist on the surface from an object for so long that the movement of water can move it.

The study involved lubrication ways that classified into three varieties of lubrication. First, bubble drag reduction is a small bubble introduced in the boundary layer. Hence it acts beneficial to reduce the turbulence momentum due to waves. Smaller bubbles assembled from the boundary layer thickness, the more effective the bubbles reduce the resistance on skin friction, according to Sanders *et al.,* [4]. Second, air layer drag reduction utilizes a constant flow of fluid so that the space within the surface of an object and the water parted to form a boundary layer presented by Ceccio [5].

Additionally, the injected air can undergo a transition and deformation from the form of bubbles into a gas. Distortion of bubbles is a vulnerability because air lubrication appears not to endure the long process of drag reduction, according to research conducted by Erick *et al.,* [6]. Twenty-five percent of the decrease in resistance that occurs when micro-sized air bubbles are used based on laboratory experiments on flat plates by Erick experiment. Amromin *et al.,* [7] also present the following deficiency in an examination with a flat plate with a total of 6m from 13 m length treated with the method, as mentioned earlier from an entire range of plate.

Lastly, partial cavity drag reduction is a gas injection method by producing a layer of lubrication between objects and fluid, creating a boundary layer. The frailty of this approach is that it provides a backflow that generates cavities in closed spaces. Gockay [8] instrument an inspection of the following method using model ships. He shows a decrease in friction force at 20 percent caused by the air cavitation layer. Based on the resulting representation, the research intended to use the first lubrication scheme to understand the extent to which nanobubble was involved in reducing drag in the flat plate experiment. Preliminary experiments Kawamura *et al.,* [9] applied air bubbles with a diameter of 0.5 mm, which two times more effective than air bubbles with a diameter of 2 mm injected in the turbulent boundary layer.

Ceccio [5] also implanted ten viscous wall unit-sized bubbles in the boundary layer, which exposes a decline in the turbidity momentum in the boundary layer. There are three main queries within the process of bubble production, bubble injection method, fluid velocity, and the size of the bubble. Overcoming these inquiries could be done by utilizing nano-sized bubbles that have the characteristics of being more difficult to dissolve in water because of the oxygen property due to the process of injection corresponding to the finding of Liu *et al.,* [10]. Meanwhile, a micro-sized bubble will be experiencing defecation because of radicals such as light, sound, micro foreign bodies. The radicals could cause a perplexity of the surface tension limit layer bubbles based on the Young-Laplace equation. The relationship between the bubble surface and the gas pressure inside and outside the bubble obtained through the Young-Laplace comparison

$$P = PI + 2\sigma / r \tag{1}$$

where σ is the surface tension, and r is the radius of the air bubble produced according to Marui [11]. Nanobubbles used in oxygen-rich drinking water treatment technology by using ceramics and carbon mixes to produce bubbles compliments the usage of reducing drag on a pipeline. Due to high effectiveness in reducing the resistance found in Kawamura *et al.,* [9] finding to produce bubbles of 0.5 to 2 mm. However, to tackle the information to find the best method of using bubble drag reduction, the research conducted must conclude the previous finding of the bubble drag reduction method.

2. Methodology

There are multiple gas injection techniques such as electrolysis, shaft plate injection, and openings structure to generate air bubbles. The research depends on an opening structure to create air bubbles. Anzai Kantetsu Co.Ltd manufactured the carbon-ceramic, which is the first structure to make nanobubble by infusing air into the small fabrications. Nanobubbles formed because of the trapped air inside the nano-sized layer. Integrated water tunnels also take place — shafts reducing restrictions to the plate lining by conveying the injected gas. The use of water tunnels as a laboratory test produces a reduction effect of 80 percent on the friction of the plate lining by Madavan [2]. These create an increase in drag reduction.

Thus, the design has faults such as bubble sliding, which depart from the surface layer, according to Elbing *et al.,* [12]. Bubble size also contributes to preventing bubble slipping. The bubble size at the same speed has also been studied and shows that air bubbles measuring 20-40 mm compared to 0.5-2 mm are more efficient, Kodama *et al.,* [3]. McCormick & Bhattacharyya [13] presented a reduction of drag by 10-30%. That proves microbubbles must be passed by fluid to perform limitation separation of microbubbles. This feature accommodated to the conditions in the research appeared in Figure 1. The unit present in Figure 2 has the following dimensions

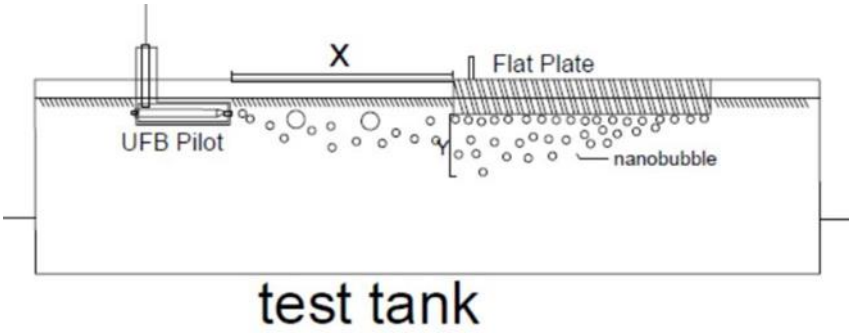

Dimensions	L: 2m, D=2m
Water Flow	20 L/min
Carbon Ceramic	8mm
Tank Capacity	200L
Piping Outer Diameter	18mm
Fluid Velocity	11m/s
Gas Pressure	0.2Mpa
Gas Distribution	60 cc/min

Fig. 1. Nanobubble containment conditions

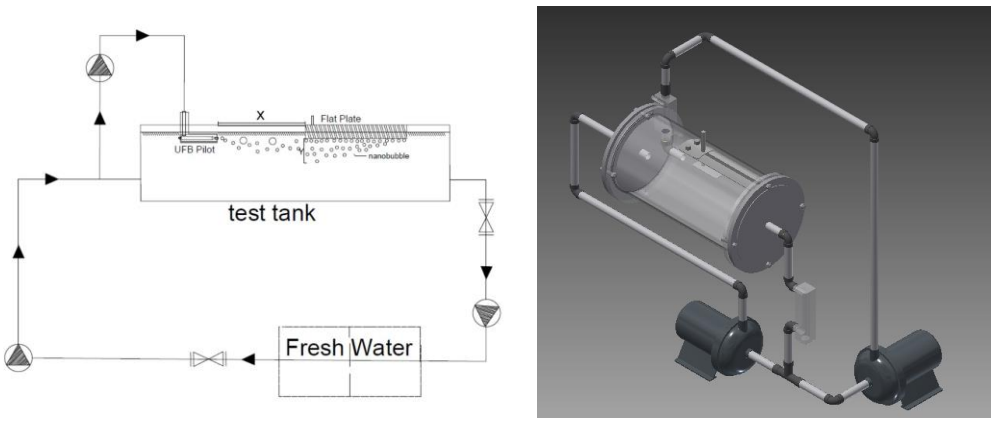

Fig. 2. Nanobubble containment unit

2.1 Experimental Procedure

The research plan is base on an investigation into two degrees conducted in the study. The first concern implies to comprehend the process of estimating air injection without nanobubble and followed by assessing air injection using nano-sized bubbles. Both experiments conducted through a series of various plates with different areas and the distance of spraying, reaching 10-100mm.

After performing the two investigations, the research produces a photographic capture to identify the gap between the plates and the boundary layer created by injecting nanobubble beneath the base. Water flow injection testing uses a pump in the exploratory vessel with pretreatment in each form of water discharge of 11 m/s without the aid of nanobubble lubrication provided with plates of varying breadths, 10mm-100mm with a difference of 10mm in each vessel. Next, perform calibrations of the scale using a micrometer ruler to specify the range in each of the graphic evidence.

Following the processing to determine a significant flow of nanobubble by creating *a mask* on the image shown by Figure 3. This single process can distinguish between nanobubble and microbubble produce in the picture. Ultimately, it is to analyze if the resulting particle from the image using the ROI Manager. The distance separating plates and working nanobubble flow subsequently measure with a ruler tools in each range of injection resulting in a y1 length in mm. Injection method obtained in 1 minute at each different plate distance and width shown by H. Sayyaadi *et al.,* [1] to see the ratio between y1, which is the contrast between boundary layer thickness and displacement thickness.

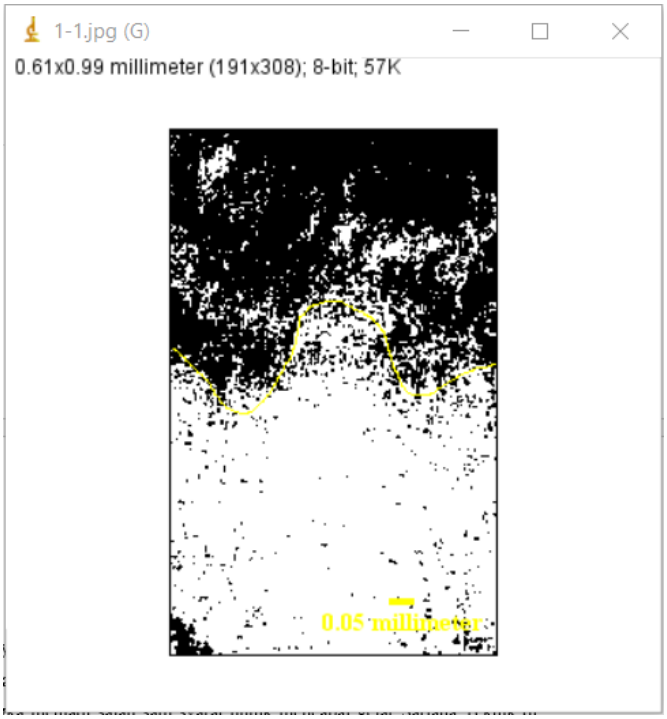

Fig. 3. Image of side view and distribution of nano bubbles with masking tools

Research held May 2019 - October 2019 at the Fluid Mechanics Technology Laboratory of the Department of Mechanical Engineering, Faculty of Engineering, University of Indonesia. The nanobubble generator unit, so-called UFB (Ultra Fine Bubble), was provided by Anzai Kantetsu Co. Ltd. Freshwater used in the following research to reduce the level of salination. However, the consequence level of the salination of liquid generates different calculation according to some studies, Kobayashi *et al.,* [14].

2.2 Governing Equation

A boundary layer (boundary layer) Blasius describes a boundary owned by a laminar limit in the form of two dimensions on a flat plate. Distinguishing flow on a flat plate when given flow and boundary layers when conditions are calm. Blasius gives two equations when the current is without a boundary layer and flow in the presence of a boundary layer. Obtained by studying the limits of physics and fluid mechanics. When the waters are calm, so there is displacement thickness occurring on the sheet of the plate to form the equation in the following manner

$$\dot{m} = \int_0^{y1} \rho_e U_e dy \tag{2}$$

$$\dot{m} = \int_0^{y1} \rho U + \rho_e U_e \delta^* \tag{3}$$

$$\rho_e = \rho \tag{4}$$

When the waters are flowing so that a boundary layer of the equation used is

$$\dot{m} = \int_0^{y1} \rho_e U_e dy = \int_0^{y1} \rho U dy + \rho_e U_e \delta^* \tag{5}$$

$$\delta^* = \frac{\int_0^{y1} (\rho_e U_e - \rho U) dy}{\rho_e U_e}, \rho = \rho_e \tag{6}$$

$$\delta^* = \int_0^{y1} (\frac{\rho_e U_e}{\rho_e U_e} - \frac{\rho U}{\rho_e U_e}) dy \tag{7}$$

$$\delta^* = \int_0^{y1} (1 - \frac{U_{(x,y)}}{U_\infty}) dy \tag{8}$$

The equation is obtained based on the momentum boundary layer equation derived from the Navier-Stock equation. With y1 as the distance between the edge of the plate and the edge of the boundary layer formed by bubble injection, U as the fluid flow velocity, and $\delta^*$the displacement thickness. Furthermore, there is a limit of the integral equation to determine as δ^* the displacement thickness and δ the thickness of the boundary layer from Blasius

$$\eta_1 = \sqrt{\frac{U_\infty}{vx}} (y1) \tag{9}$$

$$R_{ex} = \frac{U_\infty x}{v} \tag{10}$$

$$y1 = \frac{\eta_1 x}{\sqrt{R_{ex}}} \tag{11}$$

$$f'(\eta) = \frac{u}{U_\infty} \tag{12}$$

The above equation defined by taking into account the boundary constants in the displacement thickness integral, v as the viscosity of the fluid, x as the distance of the plate to the injection pipe, and R_{ex}as the Reynold number. The equation is useful as a boundary of the integral in displacement thickness which later defined in the following equation

$$\delta^* = \int_0^{\eta 1}(1 - f'(\eta))d\eta \frac{x}{\sqrt{R_{ex}}} \quad (13)$$

$$\delta = \frac{4.9x}{\sqrt{R_{ex}}} \quad (14)$$

The width of the boundary layer δ is obtained based on the example that the velocity of *u* on the boundary layer reaches 0.99 U_∞ the boundary layer reaches the maximum plate edge. Putkammer calculates the integral limit η = 4.9 because, with the limitations of measurement and calculation tools, the research limits the thickness of the boundary layer as above. After experiencing knowing the two components of the equation above, it can be calculated gas flux injection and volume flux from the fluid. Based on the equation proposed by Schlinting [15] regarding the boundary layer during turbulent flow conditions and the optimum use of an air lubrication injection using a bubble can be ascertained at Q_w=α =1, due to under these conditions the bubble is in the same position as the boundary layer on the plate

$$Q_a = A.v \quad (15)$$

$$Q_w = U_\infty(\delta - \delta^*).W_{plate} \quad (16)$$

$$\alpha = \frac{Q_a}{Q_w} \quad (17)$$

2.3 Correction Factor

The research tank kept for 2 hours difference from the previous research process based on the resulting nanobubbles that will disappear entirely from the experimental tube. The possibility of the error caused by detailed measurements from research must be minimized, and a correction factor is needed to justify the calculation. Based on research produced by Durst [16] regarding heating of cables to calculate correction factors for boundary layer studies. It is described as a limit of 2 conditions, namely when Y^+ is above four and below or equal to four and A, B are the factor of the found coefficient

$$y^+ > 4 \xrightarrow{so} Cf = 1 \quad (18)$$

$$y^+ \leq 4 \xrightarrow{so} Cf = 1 - e^{Ay^+B} \quad (19)$$

3. Results

3.1 Result and Measurement

The interaction obtained from the formation process required when conducting data collection; There are defined limits such as water density, airflow velocity, water flow velocity, and distance used at a particular flow velocity. The experiment carried in an approved flow speed of 11m/s. The density of the water used is 997 kg/m3. In addition to the mass of water, there is a water viscosity of 1,827 Pa·s. Flow rates applied in water produce a Reynold number of 40300. The flow makes assessing measures on the y-axis easier because there implies a stable flow in the scattering bubble against the flat plate. The data generated can be seen in the discussion below.

3.1.1 Without nanobubble

The corresponding data result, including standard, is not affected by the presence of nano-sized bubbles on a flat plate. In 2 dimensions, the X-axis does not change the frequency of bubbles on flat plates. The inquiry carried out on the aspect with the Y-axis proposed by Blasius authenticates that particular estimation method. However, this discussion carried out on flow by not using nano-sized bubbles to decentralize the course of ordinary water flowing on a flat plate at a speed of 11m/s. In the first stage, data used in the distribution of nanobubble beneath the slab with a width of 10mm to 100mm — the following results obtained in Figure 4.

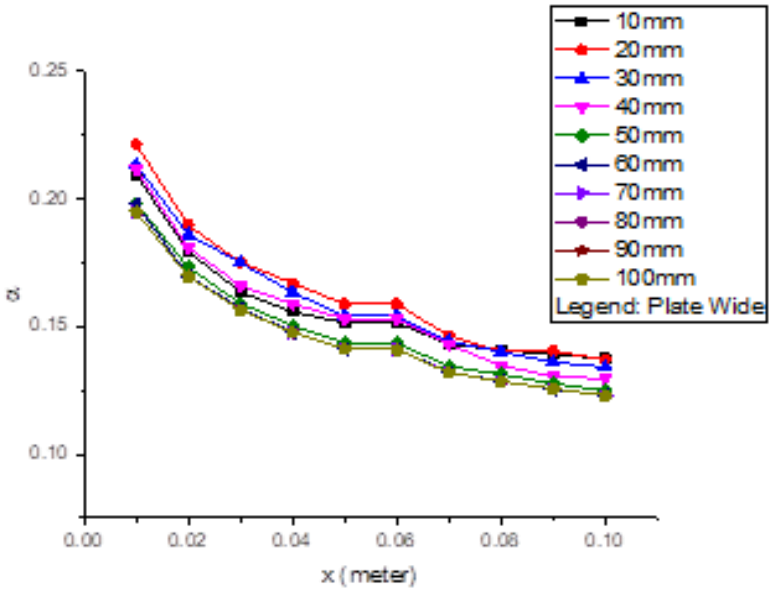

Fig. 4. Table air injection rate vs distance of injection without nanobubble

The impact of boundary layer spacing does not have a substantial effect on the local void ratio produced. However, seen when x = 80mm up to 100mm, the estimation of air injection reaches 0.786. Yet, it confirmed in theory that the closer to the estimated air injection up to 1, the more compelling the flow would be. By using nanobubbles, speed up the process of achieving dose estimation, reaching 1 with a smaller plate width with a longer distance — the resulting y-axis in Figure 5.

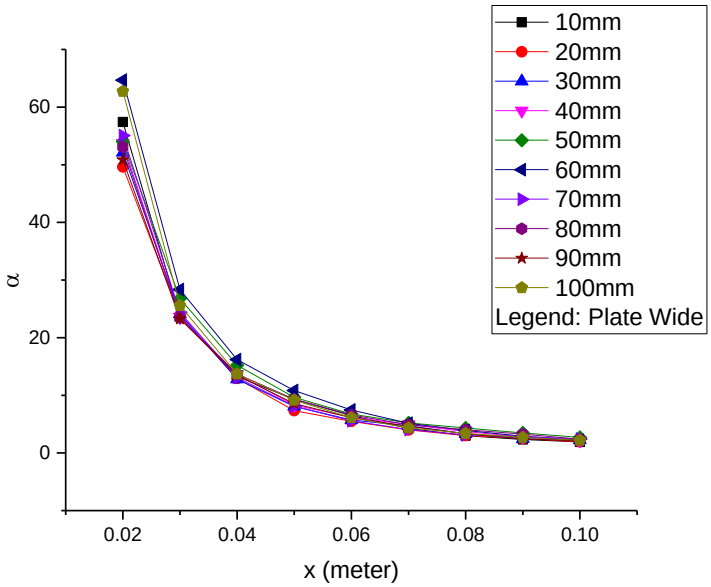

Fig. 5. Table air injection rate vs. distance of injection with nanobubble

3.1.2 With nanobubble

Nanobubbles produce a variety of differences in graphs. The graphs are the result of the ratio between the width to distance ratio used to perform nanobubble injection at the boundary layer and the ratio of the resulting air injection rate. The multiplier generated is increased by the Blasius equation through the plate surface, which is 0.82912. As can be seen in the graph presented below, there is an increasingly efficient air injection so that the study results in injection optimization using nano-sized bubbles.

$$Q_W = \beta . U_\infty . W_{plate} . {R_{ex}}^{0.2} \tag{20}$$

$$Q_W = \beta . {L_{plate}}^{0.8} . v^{0.2} . V^{0.8} . W_{plate} \tag{21}$$

$$0.82912 = \frac{Q_a}{\alpha . {L_{plate}}^{0.8} . v^{0.2} . V^{0.8} . W_{plate}} \tag{22}$$

Furthermore, the experiment discovered a resulting injection position. The optimum injection ratio has a 20mm full base, and with a distance close to 100mm, seen in the photographic evidence produced at the next point. X-Axis or the length of the plates used does not affect. Supported by research proposed by Putkammer and Kodama *et al.,* the relationship graph between the width and the estimated air injection ratio produced can be analyzed using Figure 6 below.

The influential flow velocity should also contribute to the distribution of nanobubbles. However, further research is needed because, in this study, we only provide correspondence data from the relationship between the width of the plate and the distance used on the plate. The distance between the boundary layer and the plated layer is not a problem because the scale characteristics of the boundary layer do not distinguish too great results. The plating layer can be used in the flow and not used in the outside flow, so the distribution effect is better and controlled.

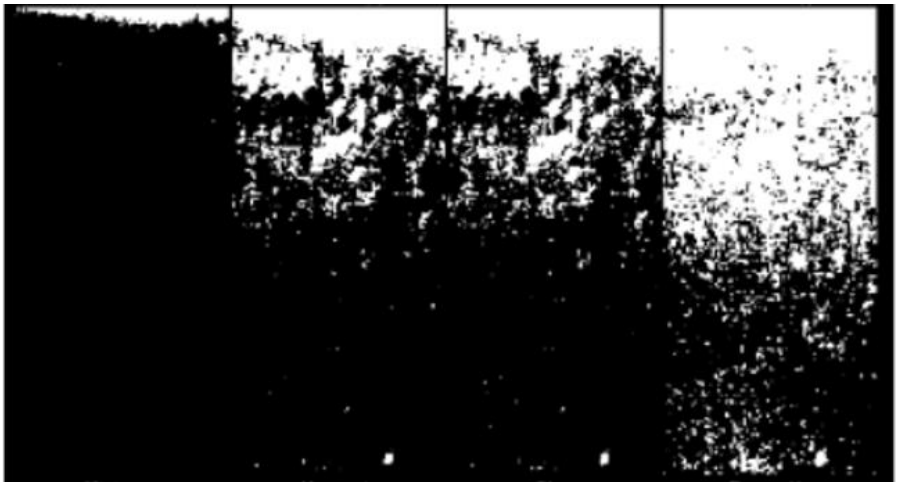

(a) (b) (c) (d)

Fig. 6. Before and after shots, (a) is before using nanobubble and (b) until (d) is after using nanobuble

3.2 Photographic Evidence

To show the presence of micro and nanoparticles so that there is no bias in the resulting image. The difference from the ROI Manager process in the images of research results. We exhibit photos of the advantage of nano-sized bubbles. Different distances could be seen, i.e., at a length of 10mm, 60mm, and 100mm, with a plate width of 20mm used as a plate width with the ideal conditions in using nanobubble injection. In the picture, at a distance of 10mm, picture b at 60mm, and picture c at a range of 100mm. In each image, shows the degradation of the resulting bubble distribution widens and sticking to the plate surface. Furthermore, at a distance of 100mm and width of 60mm, the ideal state is formed because the distribution evenly distributed, and no bubbles are colliding with other bubbles so that the resulting product does not experience an eruption. The photo took at a speed of 11m/s; this speed obtained when the injector was used right at the boundary layer produced in the plate surface layer.Furthermore, it has shown from Figure 7 that there is a flow transition produced. From the flow, which is the distribution of bubbles or BDR to Figure 7(c), it has shown that the bubbles are not too visible so that they become ALDR. The decrease ineffectiveness of the use of bubbles originates when the distance is below 100mm.

Moreover, it has proved from Figure 7 that there is a current transition composed. From the course, which is the distribution of bubbles or BDR to Figure 7(c), it has shown that the bubbles are not too visible so that they become ALDR. Decrease ineffectiveness use bubbles originate when the distance is below 100mm and at the beginning of 10mm, where the bubble is crashing through each other forming microbubble.

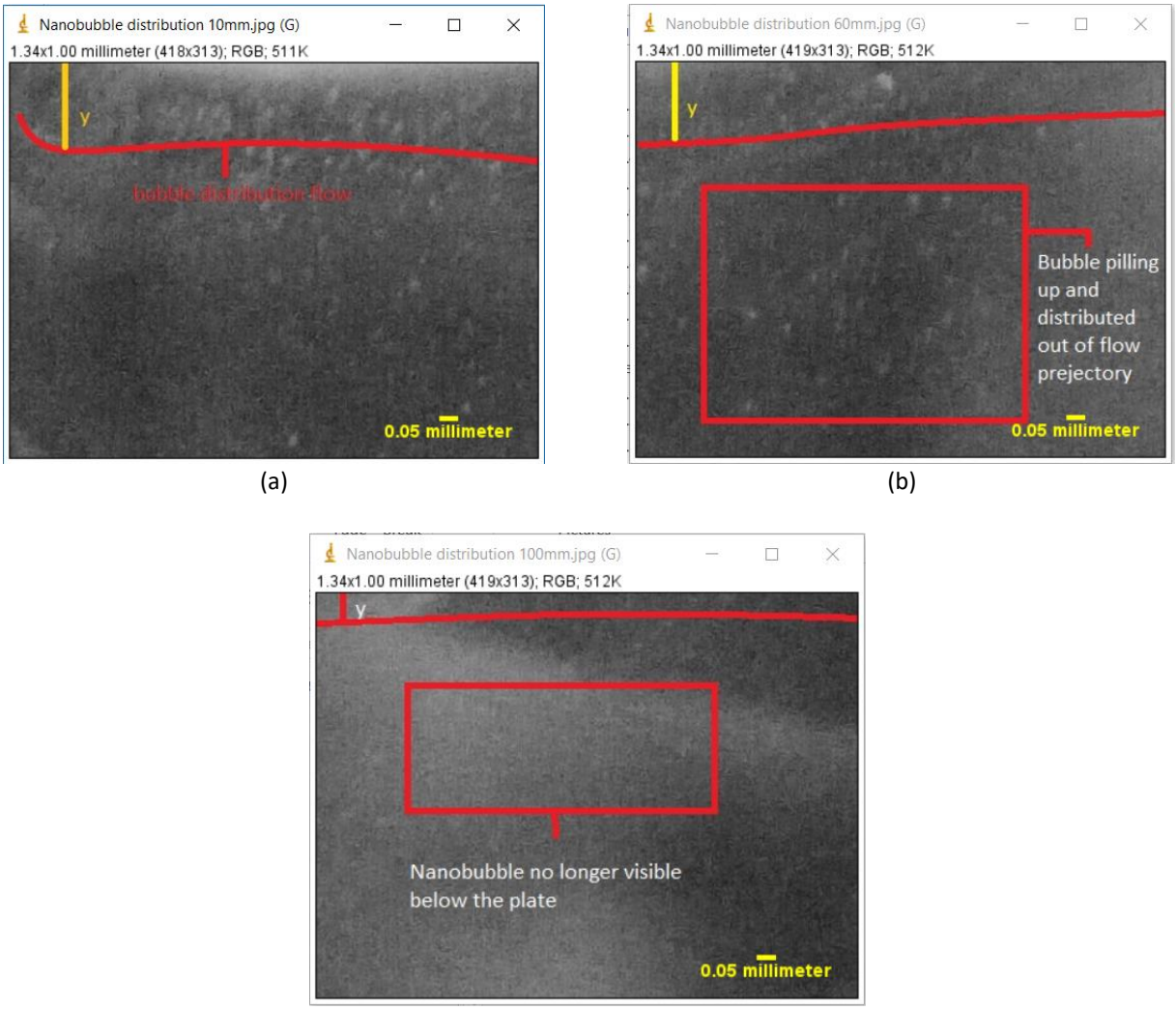

Fig. 7. Nanobubble distribution at V= 11m/s (a) Y distance calculation at 10mm (b) Y distance calculation at 60mm (c) Y distance calculation at 100mm

4. Conclusions

The nano bubble interaction on flat plate was investigated. The followings are the conclusions

i. The local void ratio is relative to 1; it is more likely to have the most significant drag reduction.
ii. The recommendation is to use a plate with a distance, a ratio of 1:0.83943, or in other words, a 1m plate requires a distance of 0.839m to inject nano-sized bubbles from the end of the plate.
iii. The multiplier factor that we appealed for when calculating the flow of water in the boundary layer was 0.82912 based on the results of the experiments conducted.
iv. Further research is carried out on its interactions with different fluids and manipulating the resulting injection holes so that different angles result in different bubble distributions. Salination also contributes to the viscosity of the fluid used in the experiment.

Acknowledgment

This research supported by Penelitian Dasar Ristekdikti 2019-2020.

References

[1] Sayyaadi, H., and M. Nematollahi. "Determination of optimum injection flow rate to achieve maximum micro bubble drag reduction in ships; an experimental approach." *Scientia iranica* 20, no. 3 (2013): 535-541.

[2] Madavan, N. K., S. Deutsch, and C. L. Merkle. "Reduction of turbulent skin friction by microbubbles." *The Physics of Fluids* 27, no. 2 (1984): 356-363.
https://doi.org/10.1063/1.864620

[3] Kodama, Yoshiaki, Akira Kakugawa, Takahito Takahashi, Satoru Ishikawa, Chiharu Kawakita, Takeshi Kanai, Yasuyuki Toda et al. "A Full-scale Experiment on Microbubbles for Skin Friction Reduction Using" SEIUN MARU"." *Journal of the Society of Naval Architects of Japan* 2002, no. 192 (2002): 1-13.
https://doi.org/10.2534/jjasnaoe1968.2002.1

[4] Sanders, Wendy C., Eric S. Winkel, David R. Dowling, Marc Perlin, and Steven L. Ceccio. "Bubble friction drag reduction in a high-Reynolds-number flat-plate turbulent boundary layer." *Journal of Fluid Mechanics* 552 (2006): 353-380.
https://doi.org/10.1017/S0022112006008688

[5] Cho, J., Marc Perlin, and Steven L. Ceccio. "Measurement of near-wall stratified bubbly flows using electrical impedance." *Measurement Science and Technology* 16, no. 4 (2005): 1021-1029.
https://doi.org/10.1088/0957-0233/16/4/015

[6] Elbing, Brian R., Eric S. Winkel, Keary A. Lay, Steven L. Ceccio, David R. Dowling, and Marc Perlin. "Bubble-induced skin-friction drag reduction and the abrupt transition to air-layer drag reduction." *Journal of Fluid Mechanics* 612 (2008): 201-236.
https://doi.org/10.1017/S0022112008003029

[7] Amromin, Eduard, Jim Kopriva, Roger EA Arndt, and Martin Wosnik. "Hydrofoil drag reduction by partial cavitation." *J. of Fluids Engineering,* no.128 (2006):931-936.
https://doi.org/10.1115/1.2234787

[8] Gokcay, S., M. Insel, and A. Y. Odabasi. "Revisiting artificial air cavity concept for high speed craft." *Ocean Engineering* 31, no. 3-4 (2004): 253-267.
https://doi.org/10.1016/j.oceaneng.2003.05.002

[9] Kawamura, Takafumi, Yasuhiro Moriguchi, Hiroharu Kato, Akira Kakugawa, and Yoshiaki Kodama. "Effect of bubble size on the microbubble drag reduction of a turbulent boundary layer." In *ASME/JSME 2003 4th Joint Fluids Summer Engineering Conference*, pp. 647-654. American Society of Mechanical Engineers Digital Collection, 2003.
https://doi.org/10.1115/FEDSM2003-45645

[10] Liu, Shu, Seiichi Oshita, Saneyuki Kawabata, Yoshio Makino, and Takahiko Yoshimoto. "Identification of ROS produced by nanobubbles and their positive and negative effects on vegetable seed germination." *Langmuir* 32, no. 43 (2016): 11295-11302.
https://doi.org/10.1021/acs.langmuir.6b01621

[11] Deutsch, Steven, Michael Moeny, Arnold Fontaine, and Howard Petrie. "Microbubble drag reduction in rough walled turbulent boundary layers." In *ASME/JSME 2003 4th Joint Fluids Summer Engineering Conference*, pp. 665-673. American Society of Mechanical Engineers Digital Collection, 2003.

[12] Elbing, Brian R., Eric S. Winkel, Keary A. Lay, Steven L. Ceccio, David R. Dowling, and Marc Perlin. "Bubble-induced skin-friction drag reduction and the abrupt transition to air-layer drag reduction." *Journal of Fluid Mechanics* 612 (2008): 201-236.
https://doi.org/10.1017/S0022112008003029

[13] McCORMICK, MICHAEL E., and Rameswar Bhattacharyya. "Drag reduction of a submersible hull by electrolysis." *Naval Engineers Journal* 85, no. 2 (1973): 11-16.
https://doi.org/10.1111/j.1559-3584.1973.tb04788.x

[14] Kobayashi, Kazuya, Yunfeng Liang, Tetsuo Sakka, and Toshifumi Matsuoka. "Molecular dynamics study of salt–solution interface: Solubility and surface charge of salt in water." *The Journal of chemical physics* 140, no. 14 (2014): 144705.
https://doi.org/10.1063/1.4870417

[15] Schlichting, Hermann, and Klaus Gersten. *Boundary-layer theory*. Springer, 2016.
https://doi.org/10.1007/978-3-662-52919-5_13

[16] Durst, F., E-S. Zanoun, and M. Pashtrapanska. "In situ calibration of hot wires close to highly heat-conducting walls." *Experiments in Fluids* 31, no. 1 (2001): 103-110.
https://doi.org/10.1007/s003480000264